Mixed-derivative skewness for high Prandtl and Reynolds numbers in homogeneous isotropic turbulence

Antoine Briard, Thomas Gomez

Mixed-derivative skewness for high Prandtl and Reynolds numbers in homogeneous isotropic turbulence

A. Briard[1] and T. Gomez[2, 3, a)]
[1)] *Sorbonne Universités, UPMC Univ Paris 06, CNRS, UMR 7190, ∂'Alembert, F-75005, Paris, France*
[2)] *Université Lille Nord de France, F-59000 Lille, France*
[3)] *USTL, LML, F-59650 Villeneuve d'Ascq, France*

(Dated: 25 August 2016)

The mixed-derivative skewness $S_{u\theta}$ of a passive scalar field in high Reynolds and Prandtl numbers decaying homogeneous isotropic turbulence is studied numerically using eddy-damped quasi-normal markovian closure, for $Re_\lambda \geq 10^3$ up to $Pr = 10^5$. A convergence of $S_{u\theta}$ for $Pr \geq 10^3$ is observed for any high enough Reynolds number. This asymptotic high Pr regime can be interpreted as a saturation of the mixing properties of the flow at small scales. The decay of the derivative skewnesses from high to low Reynolds numbers and the influence of large scales initial conditions are investigated as well.
Vol. 28 (8) 081703

The complete understanding of passive scalar mixing in turbulent flows is a challenging topic of great interest for theoretical and practical considerations. Even in the classical framework of homogeneous isotropic turbulence (HIT), there are still open questions regarding the influence of the Prandtl number Pr (or Schmidt number Sc), which is the ratio of the kinematic viscosity ν to the thermal (molecular) diffusivity ν_θ, on the scalar dynamics. Indeed, the Prandtl number strongly affects the small and very small scales of the scalar variance spectrum $E_\theta(k,t)$, as discovered by Batchelor[1] pioneering work. In recent studies[2,3], the impacts of the Prandtl number on both the passive scalar decay and on the scalar spectrum small scales have been studied. The main conclusion was that whatever the Prandtl number is, it has no major impact on the scalar decay laws provided by the Comte-Bellot and Corrsin[4] theory, which relies on dimensional analysis. However, third-order statistics were not studied, which motivates the present work.

The case $Pr \gg 1$ is of particular interest for various reasons. It specifically corresponds to the framework of biological fluids[5] (low temperature dissolved oxygen where $Sc \simeq 1000$, crucial for marine ecosystems), of chemical reactions (reduction of ferricyanide for instance, where Sc can exceed 10^4) and of experiments with tracers (such as disodium fluorescein where $Sc \simeq 2000$, or sulforhodamine 101 where $Sc \simeq 5000$). Beyond these practical considerations, the case of weakly diffusive passive scalars is challenging as it presents some difficulties in direct numerical simulations (DNS) when it comes to solve the very small scales of the scalar field beyond the Kolmogorov wavenumber k_η. These small scales experience friction by the Kolmogorov scale velocity field, up to the Batchelor wavenumber $k_B = \sqrt{Pr}k_\eta$. This continuous friction creates the viscous-convective range[1], where the scalar variance spectrum $E_\theta(k,t)$ scales as

$$E_\theta(k,t) = \frac{K_0}{3}\epsilon_\theta\sqrt{\frac{\nu}{\epsilon}}k^{-1}, \qquad k_\eta < k < k_B, \tag{1}$$

where ϵ and ϵ_θ are the kinetic energy and scalar variance dissipation rates, and $K_0 \simeq 1.4$ is the Kolmogorov constant. The framework of HIT (with or without a mean scalar gradient) with $Pr \gg 1$ has already received some attention, especially numerically[6–9], and the k^{-1} viscous-convective range has been assessed numerous times. However in DNS, with an increasing Pr comes a diminishing Reynolds number based on the Taylor micro-scale Re_λ. Furthermore, at moderate Reynolds numbers, the spatial resolution beyond the Kolmogorov wavenumber can be questioned. Notably, it has been pointed out in a recent work[10] of forced isotropic turbulence, that both the Reynolds number and the resolution are of great importance: especially, at a given Reynolds number, a better spatial resolution, of order k_B^{-1}, improves local isotropy. The same conclusion is made at constant resolution for an increasing Re_λ. A scalar field with a low diffusivity has also been studied experimentally[11–13] (often with dye, where $Sc \sim 10^3$) at higher Reynolds numbers, but the framework is hardly homogeneous and isotropic (jets, shear flows, ...).

Therefore, the present study is performed in HIT with the eddy-damped quasi-normal markovian (EDQNM) closure[14], which permits to reach both large Reynolds and Prandtl numbers. Moreover, EDQNM has been used recently[15,16] to study third-order moments of the velocity field, especially the velocity derivative skewness S. Here, the emphasis is put on the mixed-derivative skewness $S_{u\theta}$, which is of great theoretical interest since it directly appears in the passive scalar equations[18]. The main evolution equations are firstly recalled along with the spectral definitions of the third-order moments of the flow. EDQNM simulations are then briefly assessed by comparison of skewnesses S

[a)] Electronic mail: thomas.gomez@univ-lille1.fr

and $S_{u\theta}$ to experimental results at $Pr \simeq 1$. Then, for $Pr \gg 1$, the k^{-1} scaling of the scalar spectrum E_θ is recovered. The influence of an increasing Prandtl number on the mixed-derivative skewness is investigated along with large scales initial conditions, and finally, numerical evidence is given for a Re_λ^{-1} scaling of both S and $S_{u\theta}$.

In the framework of homogeneous isotropic turbulence, where a passive scalar θ is convected by a turbulent velocity field u_i, the starting point is the exact Lin equation

$$\frac{\partial E_{(\theta)}}{\partial t} + 2\nu_{(\theta)} k^2 E_{(\theta)}(k,t) = T_{(\theta)}(k,t). \tag{2}$$

The subscript $()_{(\theta)}$ refers to the scalar field. E and E_θ are the kinetic energy and scalar variance spectra, k is the wavenumber, and T and T_θ are the non-linear isotropic transfers which are explicitly computed by EDQNM (see Ref[14] for details on the closure). The turbulent kinetic energy and scalar variance, and their respective dissipation rates are defined as $K_{(\theta)}(t) = \int_0^\infty E_{(\theta)}(k,t)dk$ and $\epsilon_{(\theta)}(t) = 2\nu_{(\theta)} \int_0^\infty k^2 E_{(\theta)}(k,t)dk$. The evolution equations of the kinetic and scalar dissipation rates can be obtained by multiplying (2) by $2\nu_{(\theta)}k^2$ and then integrating over k

$$\frac{\partial \epsilon_{(\theta)}}{\partial t} = 2\nu_{(\theta)} \int_0^\infty k^2 T_{(\theta)}(k,t)dk - 4\nu_{(\theta)}^2 \int_0^\infty k^4 E_{(\theta)}(k,t)dk. \tag{3}$$

Using the turbulent Reynolds number $Re_T = K^2/(\nu\epsilon) = 3Re_\lambda^2/20$, and the Reynolds number Re_λ based on the Taylor microscale $\lambda = \sqrt{10K\nu/\epsilon}$, classical algebraic derivation[18,19] yields

$$\frac{\partial \epsilon}{\partial t} = -\left(\frac{7}{3\sqrt{15}} S(t)\sqrt{Re_T} + \frac{7}{15}G(t)\right)\frac{\epsilon^2}{K} = -\frac{7}{15}\left(\frac{1}{2}S(t)Re_\lambda + G(t)\right)\frac{\epsilon^2}{K}, \tag{4}$$

where $S(t)$ and $G(t)$ are the velocity derivative skewness and palinstrophy respectively

$$S(t) = \frac{<(\partial u/\partial x)^3>}{<(\partial u/\partial x)^2>^{3/2}} = -\frac{3\sqrt{30}}{14}\frac{\int_0^\infty k^2 T(k,t)dk}{\left(\int_0^\infty k^2 E(k,t)dk\right)^{3/2}}, \tag{5}$$

$$G(t) = <u^2>\frac{<(\partial^2 u/\partial x^2)^2>}{<(\partial u/\partial x)^2>^2} = \frac{30\nu}{7}\frac{K}{\epsilon}\frac{\int_0^\infty k^4 E(k,t)dk}{\int_0^\infty k^2 E(k,t)dk}, \tag{6}$$

where u is the component of the velocity field along the x axis. Similarly, for the passive scalar field, one gets

$$\frac{\partial \epsilon_\theta}{\partial t} = -\left(\sqrt{\frac{5}{3}} S_{u\theta}(t)\sqrt{Re_T} + r\frac{5}{9}G_\theta(t)\right)\frac{\epsilon\epsilon_\theta}{K} = -\left(\frac{1}{2}S_{u\theta}(t)Re_\lambda + r\frac{5}{9}G_\theta(t)\right)\frac{\epsilon\epsilon_\theta}{K}, \tag{7}$$

where r is the kinetic to scalar time scales ratio $r = (K\,\epsilon_\theta)/(K_\theta\,\epsilon)$. These evolution equations (4) and (7) have already been obtained in previous works[16–18] in a similar manner. This numerical study focuses on the mixed-derivative skewness

$$S_{u\theta}(t) = \frac{<(\partial u/\partial x)(\partial\theta/\partial x)^2>}{\sqrt{<(\partial u/\partial x)^2>}<(\partial\theta/\partial x)^2>} = -\sqrt{\frac{3}{10}}\frac{\int_0^\infty k^2 T_\theta(k,t)dk}{\sqrt{\int_0^\infty k^2 E(k,t)dk}\left(\int_0^\infty k^2 E_\theta(k,t)dk\right)}, \tag{8}$$

which directly appears in equation (7). Note that we obtain a factor $\sqrt{3/10}$, instead of $2/\sqrt{15}$ proposed by Antonia and Orlandi[20]. The scalar palinstrophy reads

$$G_\theta(t) = <\theta^2>\frac{<(\partial^2\theta/\partial x^2)^2>}{<(\partial\theta/\partial x)^2>^2} = \frac{18\nu_\theta}{5}\frac{K_\theta}{\epsilon_\theta}\frac{\int_0^\infty k^4 E_\theta(k,t)dk}{\int_0^\infty k^2 E_\theta(k,t)dk}. \tag{9}$$

The kinetic and scalar palinstrophy G and G_θ can be interpreted as the dissipation of the gradients of the velocity and scalar fields respectively[19], and more specifically, G represents the dissipation of enstrophy $<\omega^2> = \epsilon/\nu$.

Now that the theoretical aspects have been recalled, numerical results are presented at various Prandtl and Reynolds numbers. The wavenumber space is discretized using a logarithmic mesh, $k_{i+1} = 10^{1/f}k_i$, where $f = 17$ points per decade. This mesh spans from $k_{\min} = 10^{-6}k_L(0)$ to $k_{\max} = 10k_B$. The use of EDQNM to study third-order statistics is validated by comparisons with moderate Re_λ experiment[17] in Figure 1a and with DNS of forced HIT[21] at higher Re_λ in Figure 4b. In the experiment, $Re_\lambda \sim 50$ and the decay exponents $K \sim t^\alpha$ and $K_\theta \sim t^{\alpha_\theta}$ are $\alpha \simeq \alpha_\theta \simeq -1.33$. As a first approximation, this corresponds to infrared exponents $\sigma = \sigma_\theta = 3$ (with $E_{(\theta)}(k < k_L, t) \sim k^{\sigma_{(\theta)}}$, where k_L is the peak of the kinetic energy spectrum): indeed, using the theoretical exponents[2] $\alpha_{(\theta)} = -2(\sigma_{(\theta)}+1)/(\sigma+3)$, and

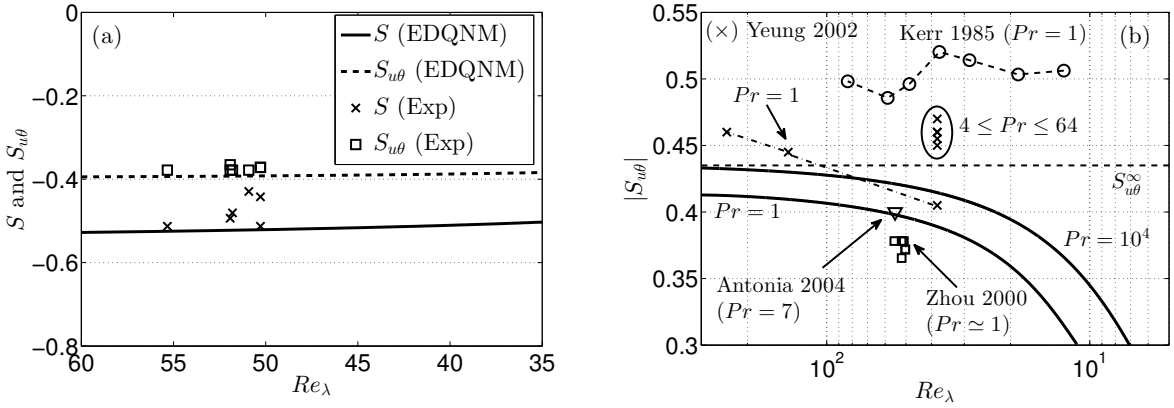

FIG. 1: (a) Comparison of S and $S_{u\theta}$ between EDQNM (lines) and experiment[17] (symbols) at $Re_\lambda \simeq 50$ and $Pr = 0.7$. (b) Review of the different values for $|S_{u\theta}|$ obtained in DNS[6,19,20] and experiments[17]: thick lines for EDQNM at $Pr = 1$ and $Pr = 10^4$. $(--)$ indicates the asymptotic Pr-state $S^\infty_{u\theta}$ at very large Re_λ and Pr. For Ref[6], Yeung 2002 $(\times)$: the values of $S_{u\theta}$ presented are in the plane perpendicular to the mean scalar gradient, the Prandtl number is $1 \leq Pr \leq 64$, and the $Pr = 1$ results are linked by a dash-dot $(-\cdot)$ line.

the measured values $\alpha_{(\theta)} \simeq -1.33$, this yields $\sigma_{(\theta)} = 2.97$. Imposing $2 \leq \sigma_{(\theta)} \leq 3$ does not change significantly the results. The comparison between experiment and EDQNM is presented in Figure 1a, where the velocity derivative and mixed-derivative skewnesses S and $S_{u\theta}$ are displayed. The agreement is better for $S_{u\theta}$ than for S, whose values obtained experimentally are more dispersed. An additional satisfactory low Re_λ comparison for $S_{u\theta}$ can be found in the Appendix B of our recent study[2]. At higher Reynolds numbers ($38 \leq Re_\lambda \leq 460$), the agreement for S between EDQNM and the DNS[21] of forced HIT is rather good, as revealed in Figure 4b: the velocity derivative skewness is quantitatively recovered within 5% on a broad range of Re_λ. Finally, Figure 1b gathers various values of $S_{u\theta}$ obtained in DNS and experiments for $Pr \geq 1$, and illustrates the noteworthy dispersion, probably due to the different kinds of forcing, whose consequences are amplified at moderate Reynolds numbers: furthermore, DNS of Kerr[19] suffers from a very low resolution. EDQNM results that will be discussed later in the text are also displayed.

Now, the impact of a high Prandtl number on the mixed-derivative skewness $S_{u\theta}$ is investigated with EDQNM. Such a framework has been studied, notably in DNS. However, this has been done only at moderate (or low) Reynolds numbers. Indeed, the more Pr increases, the more additional points are necessary to describe the very small scales of the scalar spectrum which behave as k^{-1} beyond the Kolmogorov wavenumber k_η, up to the Batchelor wavenumber k_B. Thanks to EDQNM closure, it is possible to reach high Reynolds numbers and high Prandtl numbers, as illustrated in Figure 2a, where the viscous-convective range predicted by Batchelor[1] grows in size with increasing Pr and spans on two decades for $Pr = 10^5$. Nevertheless, because of the logarithmic discretization, elongated triads are not taken into account, as intensively discussed in the past decades[14]. Consequently, it is necessary to add non-local contributions T^{NL}_θ to the scalar non-linear transfers T_θ of (2). Since numerical simulations show that the non-local expansions for the velocity field are negligible compared to the local transfers, only scalar non-local expansions are used. The scalar non-local flux is then

$$\Pi^+_\theta(k,t) = \left[\frac{2}{15}k\left(2E_\theta(k) - k\frac{\partial E_\theta}{\partial k}\right)\int_0^{ak}\theta^T_{kkq}q^2E(q)dq + \frac{1}{4}E(k)\int_0^{ak}\theta^T_{kkq}q^3E(q)dq - \frac{1}{4}\frac{E(k)E_\theta(k)}{k^2}\int_0^{ak}\theta^T_{kkq}q^5dq\right]$$
$$- \left[\frac{4}{3}\int_0^k k'^2E_\theta(k')\Big(\int\limits_{\sup(k,k'/a)}^{\infty}\theta^T_{k'pp}E(p)dp\Big)dk' + \frac{4}{3}\int_0^k k'^4\Big(\int\limits_{\sup(k,k'/a)}^{\infty}\theta_{k'pp}\frac{E_\theta(p)E(p)}{p^2}dp\Big)dk'\right], \qquad (10)$$

where time-dependence is omitted in the right hand side for the sake of clarity, θ^T_{kpq} is the characteristic damping time of the scalar third-order correlations which contains the eddy-damping factors[2,14], and k, p, q are the modulus of the wavectors $\boldsymbol{k}$, $\boldsymbol{p}$, $\boldsymbol{q}$ which are such that $\boldsymbol{k}+\boldsymbol{p}+\boldsymbol{q} = \boldsymbol{0}$. The interactions are non-local when $\inf(k,p,q)/\sup(k,p,q) \leq a$, where $a = 10^{1/f} - 1$ is called the nonlocality parameter[14]. The first bracket is dominant and yields the k^{-1} viscous-range for $Pr \gg 1$: it corresponds to a non-local flux from very large to very small scales, where $q/k \ll 1$, and the second bracket to a non-local flux in the opposite direction where $k/p \ll 1$. The non-local transfer is then $T^{(NL)}_\theta = -\partial_k\Pi^{(NL)}_\theta$. The impact of the non-local scalar flux is illustrated in Figure 2b at $Pr = 10^5$: it brings energy

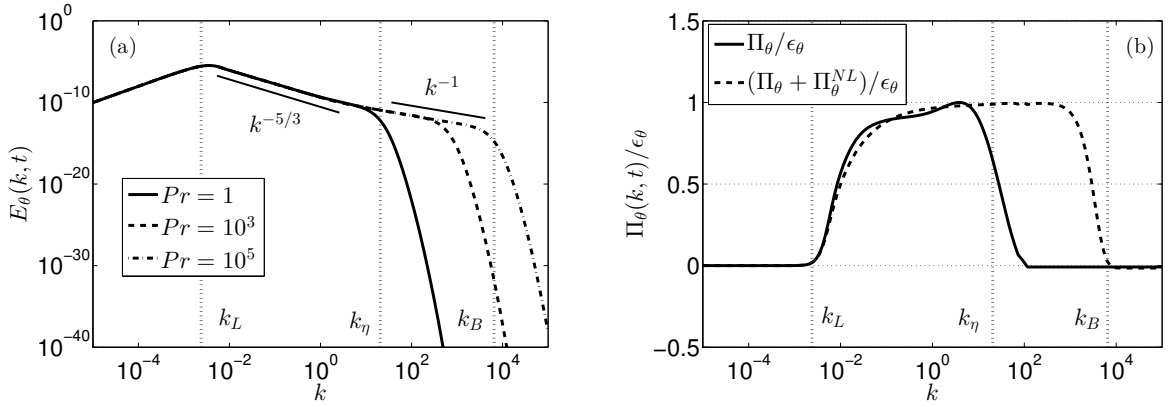

FIG. 2: (a): scalar spectrum $E_\theta(k,t)$ for various Prandtl numbers $Pr = 1$, 10^3 and 10^5. The inertial convective $k^{-5/3}$ and viscous-convective k^{-1} ranges are displayed as well, along with the integral, Kolmogorov and Batchelor wavenumbers k_L, k_η and k_B for $Pr = 10^5$. (b): normalized scalar flux $\Pi_\theta(k,t)/\epsilon_\theta$ for $Pr = 10^5$. Π_θ $(-)$ corresponds to the local scalar flux, and $\Pi_\theta^{\rm tot} = \Pi_\theta + \Pi_\theta^{NL}$ $(--)$ to the total scalar flux including the non local part. Both at $Re_\lambda = 10^3$ in Saffman turbulence ($\sigma = \sigma_\theta = 2$).

beyond the Kolmogorov wavenumber k_η and sustains the viscous-convective range. The resulting total scalar flux $\Pi_\theta^{\rm tot} = \Pi_\theta + \Pi_\theta^{NL}$ is still conservative, since $\Pi_\theta^{\rm tot}(k=0) = \Pi_\theta^{\rm tot}(k > k_B) = 0$.

The Pr-dependence of the mixed-derivative skewness $S_{u\theta}$ is investigated in Figure 3 in the high Reynolds numbers regime to avoid transitional effects towards low Reynolds numbers. It is revealed that $|S_{u\theta}|$ increases from $Pr = 1$ to a critical Prandtl number $Pr_c = 10$ and then slightly decreases up to $Pr = 10^3$. Such variations of $|S_{u\theta}|$ for $1 \leq Pr \leq 10^3$ have already been observed in DNS[6,8]. The latter works, at moderate Reynolds numbers, indicate that the decrease of $|S_{u\theta}|$ happens from $Pr_c \simeq 1$, which is smaller than in our high Reynolds numbers simulations where the decrease starts around $Pr_c \simeq 10$. Consequently, these observations suggest that the decay threshold for $|S_{u\theta}|$ is Reynolds dependent, with $Pr_c \in [1, 10]$.

The remarkable feature is that for $Pr \geq 10^3$ at high Reynolds numbers, the mixed-derivative skewness saturates to a constant value $|S_{u\theta}^\infty| \simeq 0.435$, which does not depend on the Prandtl number anymore. The ∞ symbol refers to the *saturated Pr-state* $Pr \geq 10^3$. DNS performed at higher values of Pr would be useful to confirm (or not) the saturation of $S_{u\theta}$ from $Pr \sim 10^3$. It is worth noting that in HIT, when the scalar field is forced with a mean scalar gradient, values of $S_{u\theta}^\perp$ (in the direction perpendicular to the gradient) are close to the present $S_{u\theta}^\infty = -0.435$: values of Ref[6] are gathered in Figure 1b, and one can note that at $Pr = 1$, $S_{u\theta}^\perp$ increases with Re_λ ($-\cdot\times$ line) similarly to the present EDQNM results.

Physically, this saturation of the mixed-derivative skewness means that the statistical mixing properties of the flow do not evolve anymore at a sufficiently high Prandtl number, for high Reynolds numbers. This can be interpreted in terms of small scales equilibrium ($k > k_\eta$), if one considers the spectral definition (8) of the mixed-derivative skewness $S_{u\theta}$. Indeed, considering a given Reynolds number, or equivalently a given dissipation rate ϵ of kinetic energy, increasing Pr leads to an indefinite extension of the viscous-convective range of E_θ toward small scales, whereas its inertial-convective range remains unchanged. Therefore, the variations of $S_{u\theta}$ when Pr increases are mainly due to the variations of the two functions appearing in the scalar integrated terms of $S_{u\theta}$: $k^2 T_\theta(k,t)$ and $k^2 E_\theta(k,t)$ for $k \in [k_\eta; k_B]$. These quantities represent respectively the production rate of mean-square temperature gradients and scalar dissipation at wavenumber k. Moreover, Figure 2b shows that the production is mainly a non-local mechanism unlike the scalar dissipation. For a sufficiently high Prandtl number, $Pr \geq 10^3$, these two integrals evolve similarly so that they balance each other. Therefore, for high Reynolds numbers, the convergence of $S_{u\theta}$ to a constant value $S_{u\theta}^\infty$ for increasing Prandtl numbers, reflects an equilibrium, occurring in the viscous-convective range, between non-local production of mean-square temperature gradients and scalar dissipation by diffusion.

A similar independence with regard to Pr can be found for the scalar palinstrophy G_θ: injecting classical scaling for E_θ in the spectral definition (9) of G_θ, and assuming that $Re_\lambda \gg 1$ and $Pr \gg 1$, yield $rG_\theta \sim Re_\lambda$. Such a result was also found by Ristorcelli[18]. Numerical simulations and experiments have shown that $r \sim \alpha_\theta/\alpha$ is a relevant approximation for the time scale ratio when the turbulence decay is algebraic. Therefore, one has $r \simeq 1$ when the kinetic energy and scalar variance decay similarly, *i.e.* when $\sigma = \sigma_\theta$ for the initial spectra considered here: this is relevant since it has been shown in a precedent work[2] that Pr does not affect the decay of scalar integrated quantities. Qualitatively, the independence of G_θ with regard to Pr provides the same physical information as our numerical

results on $S_{u\theta}$: there is an asymptotic convergence of the mixing properties of the passive scalar field only for a sufficiently high Pr. As said before, a dependance on Pr for moderate Prandtl numbers, say $1 \leq Pr \leq 10^3$, is in agreement with DNS[6,8].

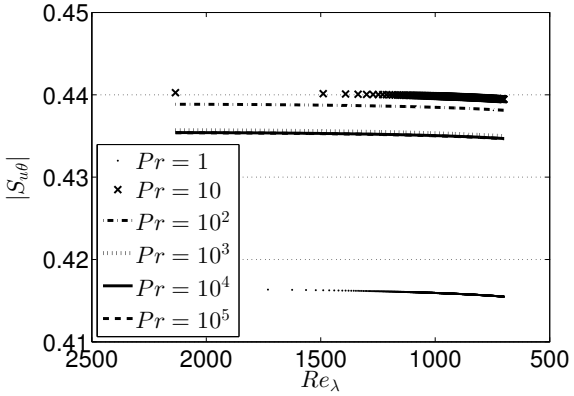

FIG. 3: Absolute value of the mixed-derivative skewness $S_{u\theta}$ for various Prandtl numbers from 1 to 10^5 in Saffman turbulence. Because of the high-Pr saturation, the $Pr = 10^4$ and $Pr = 10^5$ curves are hardly distinguishable.

Finally, the decay of the derivative skewness $S(t)$ and mixed-derivative skewness $S_{u\theta}(t)$ from high to low Reynolds numbers is investigated in Figure 4a for Saffman ($\sigma = \sigma_\theta = 2$) and Batchelor ($\sigma = \sigma_\theta = 4$) turbulence. The main results are the following ones: (i) Both S and $S_{u\theta}$ are constant for high Reynolds and Prandtl numbers, and independent of large scales initial conditions: indeed, the curves are identical for Saffman and Batchelor turbulence, except in the transition zone between the high and low Reynolds numbers regimes, where a slight difference is observed. (ii) The transition toward the low Reynolds numbers regime for the scalar field starts after the one for the velocity field, which is logical as the Péclet number $Pe_\lambda = PrRe_\lambda$ is much larger than Re_λ in the case $Pr \gg 1$. (iii) For very low Reynolds numbers, both derivative skewnesses S and $S_{u\theta}$ are zero, consistent with the fact that for $Re_\lambda < 1$, the flow is not turbulent anymore and thus there is no turbulent mixing at all.

One also has to point out that both S and $S_{u\theta}$ increase during the decay, *i.e.* when the Reynolds number decreases, in agreement with George[22]. Moreover, it is stated in the latter work that at some point during the decay, S should behave as Re_λ^{-1} according to dimensional considerations. Assuming that the Taylor micro-scale λ is the relevant similarity length scale, and using self-preserving functions $E(k,t) = E^s(t)f(\eta)$, $T(k,t) = T^s(t)g(\eta)$, and $\eta = k\lambda$, one obtains

$$S(t) \sim \frac{\lambda^{-4}\nu u^2}{(\lambda^{-2}u^2)^{3/2}} \frac{\int \eta^2 g(\eta)d\eta}{\left(\int \eta^2 f(\eta)d\eta\right)^{3/2}} \sim Re_\lambda^{-1}. \tag{11}$$

But this scaling is not always clearly observed. We believe this might be the consequence of too low Reynolds numbers in DNS. A low Reynolds defect is in agreement with the work of Schumacher *et.al.*[23], where Figure 1 herein clearly shows that the Re_λ^{-1} scaling is achieved for high Reynolds numbers only ($10^2 \leq Re_\lambda \leq 10^3$).

In Figure 4b, relevant correlations are presented (with constants determined by least square fit, set to match with the beginning of the transition) with a clear Re_λ^{-1} dependency for both the velocity derivative and mixed-derivative skewnesses. These correlations $S(t) = S^\infty + 2.145Re_\lambda^{-1}$ and $S_{u\theta}(t) = S_{u\theta}^\infty + 0.735Re_\lambda^{-1}$, where $S^\infty = -0.569$ and $S_{u\theta}^\infty = -0.435$, capture well the beginning of the transition zone. Hence, the scaling proposed by George $S \sim Re_\lambda^{-1}$ seems relevant mainly for high Reynolds numbers.

Moreover, an interesting result, never confirmed previously to our knowledge, is that the mixed-derivative skewness $S_{u\theta}$ scales in Re_λ^{-1} as well. This scaling is in agreement with another work of George[24] where similarity assumptions were used for temperature fluctuations: $E_\theta(k,t) = E_\theta^s(t)f_\theta(\eta)$, $T_\theta(k,t) = T_\theta^s(t)g_\theta(\eta)$, and $\eta_\theta = k\lambda_\theta$. Using a classical result[17,24] linking the ratio of the kinetic and scalar Taylor lengths λ and $\lambda_\theta = \sqrt{6\nu_\theta K_\theta/\epsilon_\theta}$ yields

$$\left(\frac{\lambda}{\lambda_\theta}\right)^2 = \frac{5}{6}rPr, \qquad S_{u\theta}(t) \sim \frac{\nu_\theta\lambda}{\lambda_\theta^2 u} \frac{\int \eta_\theta^2 g_\theta(\eta_\theta)d\eta_\theta}{\sqrt{\int \eta^2 f(\eta)d\eta \int \eta_\theta^2 f_\theta(\eta_\theta)d\eta_\theta}} \sim rRe_\lambda^{-1}. \tag{12}$$

In conclusion, the mixed-derivative skewness $S_{u\theta}$ has been investigated in the classical framework of decaying homogeneous isotropic turbulence, at both high Reynolds and Prandtl numbers thanks to the eddy-damped quasi-

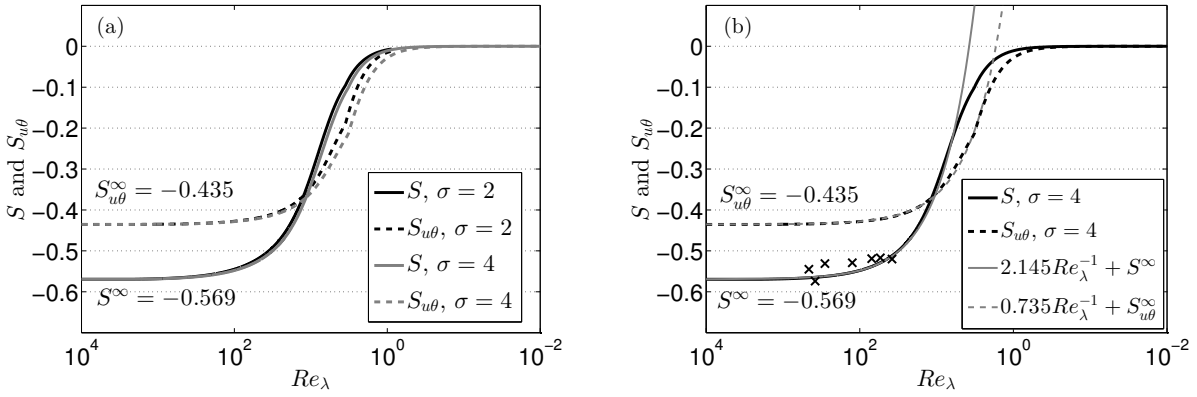

FIG. 4: Velocity derivative and mixed-derivative skewnesses S and $S_{u\theta}$ from high to low Reynolds numbers in the saturated Pr-state at $Pr = 10^4$. (a) In black for Saffman turbulence $\sigma = \sigma_\theta = 2$, and in grey for Batchelor turbulence $\sigma = \sigma_\theta = 4$. (b) Batchelor turbulence: correlations in grey that capture well the high Reynolds numbers regime and the beginning of the transition zone. $\times$: values of S from forced turbulence DNS[21].

normal markovian (EDQNM) closure. This work extends existing results obtained in direct numerical simulations at moderate Reynolds numbers and at a maximum of $Pr \simeq 10^3$. The main results of this study are twofold. Firstly, at high Reynolds numbers and for $Pr \geq 10^3$, $S_{u\theta}$ saturates to a constant value $S^\infty_{u\theta} = -0.435$, independent of the large scales initial conditions σ and σ_θ, which means that statistical properties of the scalar mixing are converged, and can be interpreted as a small scales equilibrium in the viscous-convective range. Moreover, such large values of the Prandtl (or Schmidt) number correspond to real fluids as pointed out in the introduction, which underlines the relevance of studying the physics of high Prandtl and high Reynolds numbers flows. Secondly, the Re_λ^{-1} scaling for $S_{u\theta}$ (and S), coming from self-similarity theory, was numerically assessed. These numerical and theoretical results exhibit some robust asymptotic states at very high Reynolds and Prandtl numbers for scalar third-order statistics.

[1]G. K. Batchelor, "Small-scale variation of convected quantities like temperature in turbulent fluid. Part 1. General discussion and the case of small conductivity," J. Fluid. Mech **5**, 113-133 (1959).
[2]A. Briard, T. Gomez, P. Sagaut, and S. Memari, "Passive scalar decay laws in isotropic turbulence: Prandtl effects," J. Fluid. Mech **784**, 274-303 (2015).
[3]A. Briard, and T. Gomez, "Passive scalar convective-diffusive subrange for low Prandtl numbers in isotropic turbulence," Phys. Rev. E **91**, 011001 (2015).
[4]G. Comte-Bellot and S. Corrsin, "The use of a contraction to improve the isotropy of a grid generated turbulence," J. Fluid. Mech **25**, 657 (1966).
[5]C. Scalo, U. Piomelli, and L. Boegman, "High-Schmidt-number mass transport mechanisms from a turbulent flow to absorbing sediments," Phys. Fluids **24**, 4178 (2012).
[6]P.K. Yeung, S. Xu, and K.R. Sreenivasan, "Schmidt number effects on turbulent transport with uniform mean scalar gradient," Phys. Fluids **14**, 4178 (2002).
[7]J. Schumacher, K.R. Sreenivasan, and P.K. Yeung, "Schmidt number dependence of derivative moments for quasi-static straining motion," J. Fluid. Mech **479**, 221-230 (2003).
[8]P.K. Yeung, S. Xu , D.A. Donzis, and K.R. Sreenivasan, "Simulations of Three-Dimensional Turbulent Mixing for Schmidt Numbers of the Order 1000," Flow, Comb. Turb. **72**, 333-347 (2004).
[9]M. S. Borgas, B. L. Sawford, S. Xu , D.A. Donzis, and P.K. Yeung, "High Schmidt number scalars in turbulence: Structure functions and Lagrangian theory ," Phys. Fluids **14**, 3888 (2004).
[10]D.A. Donzis and P.K. Yeung, "Resolution effects and scaling in numerical simulations of passive scalar mixing in turbulence," Physica D **239**, 1278-1287 (2010).
[11]K. A. Buch and W. J. A. Dahm, "Experimental study of the fine-scale structure of conserved scalar mixing in turbulent shear flows. Part 1. $Sc \geq 1$," J. Fluid. Mech **317**, 21-71 (1996).
[12]P. L. Miller and P. E. Dimotakis, "Measurements of scalar power spectra in high Schmidt number turbulent jets," J. Fluid. Mech **308**, 129-146 (1996).
[13]T. M. Lavertu, L. Mydlarski, and S. J. Gaskin, "Differential diffusion of high-Schmidt-number passive scalars in a turbulent jet," J. Fluid. Mech **612**, 439-475 (2008).
[14]M. Lesieur, *Turbulence in Fluids*, (Springer, New York, 2008).
[15]W. J. T. Bos, L. Chevillard, J. F. Scott, and R. Rubinstein, "Reynolds number effect on the velocity increment skewness in isotropic turbulence," Phys. Fluids **24**, 015108 (2012).
[16]M. Meldi and P. Sagaut, "Further insights into self-similarity and self-preservation in freely decaying isotropic turbulence," J. Turbulence **14**, 24-53 (2013).
[17]T. Zhou, R. A. Antonia, L. Danaila, and F. Anselmet, "Transport equations for the mean energy and temperature dissipation rates in grid turbulence," Exp. Fluids **28**, 143-151 (2000).

[18]J. R. Ristorcelli, "Passive scalar mixing: Analytic study of time scale ratio, variance, and mix rate," Phys. Fluids **18**, 075101 (2006).
[19]R. M. Kerr, "Higher-order derivative correlations and the alignment of small-scale structures in isotropic numerical turbulence," J. Fluid. Mech **153**, 31-58 (1985).
[20]R. A. Antonia and P. Orlandi, "Similarity of decaying isotropic turbulence with a passive scalar," J. Fluid. Mech **505**, 123-151 (2004).
[21]T. Gotoh, D. Fukayama, and T. Nakano, "Velocity field statistics in homogeneous steady turbulence obtained using a high-resolution direct numerical simulation," Phys. Fluids **14**, 1065-1081 (2002).
[22]W. K. George, "The decay of homogeneous isotropic turbulence ," Phys. Fluids A **4**, 1492 (1992).
[23]J. Schumacher, K. R. Sreenivasan, and P. K. Yeung, "Derivative moments in turbulent shear flows," Phys. Fluids **15**, 84 (2003).
[24]W. K. George, "Self-Preservation of Temperature Fluctuations in Isotropic Turbulence," Studies in Turbulence, 514-528 (1992).